Zoology 117 (2014) 337–348

Contents lists available at ScienceDirect

Zoology

journal homepage: www.elsevier.com/locate/zool

Locomotion of free-swimming ghost knifefish: anal fin kinematics during four behaviors

Eric D. Youngerman*, Brooke E. Flammang, George V. Lauder

Museum of Comparative Zoology, Harvard University, 26 Oxford Street, Cambridge, MA 02138, USA

ARTICLE INFO

Article history:
Received 13 March 2014
Accepted 7 April 2014
Available online 12 June 2014

Keywords:
Fish locomotion
Swimming behaviors
Fin kinematics
Fin rays
Knifefish

ABSTRACT

The maneuverability demonstrated by the weakly electric ghost knifefish (*Apteronotus albifrons*) is a result of its highly flexible ribbon-like anal fin, which extends nearly three-quarters the length of its body and is composed of approximately 150 individual fin rays. To understand how movement of the anal fin controls locomotion we examined kinematics of the whole fin, as well as selected individual fin rays, during four locomotor behaviors executed by free-swimming ghost knifefish: forward swimming, backward swimming, heave (vertical) motion, and hovering. We used high-speed video (1000 fps) to examine the motion of the entire anal fin and we measured the three-dimensional curvature of four adjacent fin rays in the middle of the fin during each behavior to determine how individual fin rays bend along their length during swimming. Canonical discriminant analysis separated all four behaviors on anal fin kinematic variables and showed that forward and backward swimming behaviors contrasted the most: forward behaviors exhibited a large anterior wavelength and posterior amplitude while during backward locomotion the anal fin exhibited both a large posterior wavelength and anterior amplitude. Heave and hover behaviors were defined by similar kinematic variables; however, for each variable, the mean values for heave motions were generally greater than for hovering. Individual fin rays in the middle of the anal fin curved substantially along their length during swimming, and the magnitude of this curvature was nearly twice the previously measured maximum curvature for ray-finned fish fin rays during locomotion. Fin rays were often curved into the direction of motion, indicating active control of fin ray curvature, and not just passive bending in response to fluid loading.

1. Introduction

Access to a three-dimensional medium with a wide diversity of habitats has resulted in the evolution of a vast array of propulsive systems in ray-finned fishes. A key feature facilitating maneuverability in ray-finned fishes is the presence of fins that extend into the water and act as control surfaces during locomotion (Lauder and Drucker, 2004; Lauder et al., 2006). Median and paired fins arrayed around the fish body and the ability of fishes to control fin movement allows fishes to vector forces during locomotion which in turn permits directional movement. One special design feature of ray-finned fish fins is active curvature control which is possible due to the bilaminar design of individual fin rays (McCutchen, 1970; Geerlink and Videler, 1986; Lauder et al., 2006; Alben et al., 2007; Taft and Taft, 2012). Ray-finned fishes can thus control the curvature of the whole fin surface by differentially moving the two distinct halves of each fin ray. Active curvature control in fins has been the subject of a number of recent experimental (e.g., Lauder et al., 2011; Taft and Taft, 2012) and kinematic studies (e.g., Lauder et al., 2006; Taft et al., 2008; Chadwell et al., 2012) which demonstrate that fishes use this ability to resist fluid loading on the fin that occurs during locomotion: by curving the fin surface *into* oncoming flow, fishes can effectively stiffen the fin and resist fin deformation that would otherwise occur.

Among the diversity of teleost fishes, one highly specialized group, the American knifefishes or Neotropical electric fishes (Teleostei: Gymnotiformes), are among the most maneuverable and possess an especially impressive fin – the elongate anal fin – that is their primary mechanism for generating locomotor forces. The anal fin can extend more than three-quarters the length of the body and be composed of nearly 340 individual fin rays in some species (Albert, 2001). This provides the capability of highly controlled wave-like fin bending patterns as well as localized conformational adaptation of fin shape to specific locomotor situations. Gymnotiform fishes, and especially the ghost knifefish, *Apteronotus albifrons*, have been used as a basis for a number of different

* Corresponding author. Tel.: +1 617 496 7199.
E-mail address: eric.youngerman@post.harvard.edu (E.D. Youngerman).

http://dx.doi.org/10.1016/j.zool.2014.04.004
0944-2006/

investigations of the anal fin propulsive system. For example, kinematic analyses of the anal fin have been conducted (Blake, 1983; Ruiz-Torres et al., 2013), the elongate anal fin has been studied as a locomotor system for analyzing how opposing forces are used to control body position (Sefati et al., 2013), fluid dynamic function of the anal fin has been studied both experimentally (Neveln et al., 2014) and computationally (Lighthill, 1990; Lighthill and Blake, 1990; Shirgaonkar et al., 2008), the role of locomotion in prey capture has been described (MacIver et al., 2001), and a novel heave (vertical) maneuvering behavior has been identified in which counter-propagating waves on the elongate anal fin generate downwardly directed forces allowing knifefish to move vertically (Curet et al., 2011a,b). And, the elongate ribbon fin of knifefish has also been used as inspiration for robotic models of wave-like locomotion (e.g., MacIver et al., 2004; Low and Willy, 2006; Hu et al., 2009; Curet et al., 2011a; Neveln et al., 2013).

In the present paper, we focus on the function of the anal fin during locomotor behaviors exhibited by free-swimming individuals, and on analyzing the relatively short duration of locomotor events that make up the typical free-swimming maneuvering characteristic of ghost knifefish, *A. albifrons*. Knifefish, moving in an unconstrained area, are very active and typically move forward, backward, in heave (vertically), and hover, and execute relatively rapid transitions among these behaviors. Previous studies of knifefish locomotion have focused for the most part on one behavior, and often in a relatively constrained experimental setting that limits maneuverability. We provide an online supplementary movie that demonstrates the complex function of the anal fin associated with unconstrained locomotion in the highly maneuverable ghost knifefish and the rapid behavioral switching that occurs among locomotor behaviors (see the supplementary video in the online Appendix). Studying locomotion under the free-swimming condition represents a qualitatively different approach than focusing on steady rectilinear flow-tank locomotion, and we emphasize in this paper (i) how anal fin function differs among locomotor behaviors, and (ii) the function and curvature of selected individual fin rays within the anal fin.

Our overall goal was to quantify how anal fin kinematic and fin ray curvature patterns change with different locomotor behaviors. Because modulation of the kinematics of a single fin is responsible for both vertical and horizontal movement, we hypothesized that anal fin kinematics necessary to produce forward, backward, heave, and hovering swimming behaviors would be accomplished by variation in the position and extent of fin ray curvature along the length of the anal fin. Furthermore, we anticipated that the direction, amplitude, and wavelength of fin undulations required to execute one behavior (e.g., forward swimming) would be different from those that produced other behaviors (e.g. backward, heave, or hover swimming). A further goal was to compare the curvatures exhibited by knifefish anal fin rays during unrestrained swimming with values measured previously in the literature in other teleost fish species during locomotion.

2. Materials and methods

2.1. Fish

Data were collected from three ghost knifefish, *A. albifrons* (Linnaeus, 1766), purchased from a local commercial supplier. Fish were maintained separately in 40 l aquaria and kept under a 12 h:12 h L:D photoperiod with a mean water temperature of $26 \pm 1\,^{\circ}C$ (mean ± standard error of the mean, s.e.). The three fish analyzed had a mean total length of 18.9 ± 0.8 cm. Fish were allowed to acclimate in the experimental tank for 15 min prior to recording any video footage.

2.2. Morphology

Anal fin morphology was investigated to aid in interpretation of fin kinematics. Superficial dissection of the musculature surrounding the anal fin was used to determine the structure of the different layers of muscle possibly involved in the movement of the anal fin. For a study of the skeleton, a cleared and stained specimen of *A. albrifrons* (specimen number MCZ# 45195; Museum of Comparative Zoology, Harvard University, Cambridge, MA, USA) was examined. For a more in-depth examination of the skeleton, X-ray computed microtomography (micro CT) scans of both an entire specimen and a small posterior section (MCZ# 169184) were analyzed in VGStudio Max version 2.0 (Volume Graphics GmbH, Heidelberg, Germany). Micro CT scans were conducted with an X-Tec HMXST 225 scanner (Nikon Metrology, Inc., Brighton, MI, USA). Each scan slice had a resolution of 920×844 pixels and we produced 1998 slides with a voxel size of 0.0586 mm along the *x*-, *y*-, and *z*-axes.

2.3. Behavioral analysis

Experiments were conducted in a 20 l glass aquarium with a water temperature of $26 \pm 1\,^{\circ}C$. Three synchronized high-speed video cameras were used to record the movement of the anal fin (two Photron Fastcam 1024×1024 pixel cameras, and a Photron APX 1024×1024 pixel system; Photron Inc., Tokyo, Japan). Videos were recorded at 1000 fps from lateral, posterior, and ventral perspectives allowing for a three-dimensional analysis of the desired kinematic parameters.

Four visually discernible locomotor behaviors were selected for kinematic analysis: forward swimming, backward locomotion, heave (vertical motion), and hover (maintaining body position in the water column). Considerable effort was devoted to identifying discrete sequences for each behavior that were of sufficient length for quantitative analysis and to ensure that sequences of one behavior were not interrupted by other movements. A forward sequence was selected if a fish's dominant movement was in the anterior direction along the horizontal axis with a minimal amount of vertical movement. A backward sequence was similarly defined but with a dominant velocity in the posterior direction along the horizontal axis. A heave sequence was selected if the fish's dominant velocity was positive along the vertical axis with a minimal amount of horizontal movement. A hover sequence was selected if a fish maintained its place in the water column (with minimal amounts of both horizontal and vertical movement). Video footage was recorded while individual knifefish swam freely. Post hoc analysis further simplified the recorded footage, selecting smaller sequences of footage that matched criteria for each behavior and had at least one complete period for that behavior. For each of the four behaviors and for each individual fish, we measured between 10 and 20 fin waves.

Kinematic sequences were calibrated in three dimensions using a calibration cube consisting of a square base and 15 precisely measured perpendicularly protruding, metal spikes, which allowed three-dimensional coordinates to be measured using conventional direct linear transformation (DLT) methods as in our previous research (e.g., Flammang and Lauder, 2009; Blevins and Lauder, 2012). Digitizing was done using a custom Matlab program (version 7.10; Mathworks, Natick, MA, USA) developed by Tyson Hedrick of the University of North Carolina at Chapel Hill (Hedrick, 2008). A second custom Matlab program was used for two-dimensional analysis of the anal fin. Between 140 and 200 points were digitized along the distal edge of the fin as well as an easily trackable body point (nostril) for each sequence analyzed (Fig. 1). This allowed quantification of the complete anal fin waveform. Three-dimensional coordinate data were exported to Microsoft Office

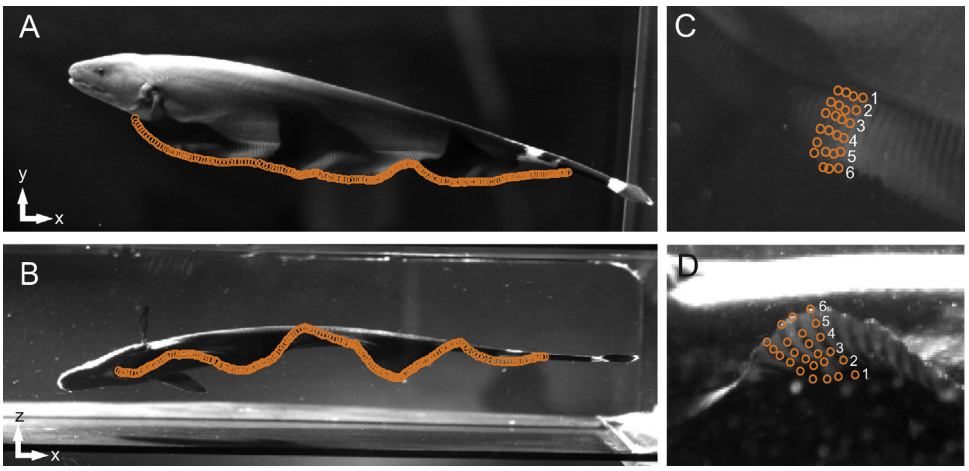

Fig. 1. (A) Lateral view of an individual ghost knifefish, *Apteronotus albifrons*, at the start of a backwards swimming sequence. (B) Ventral view of the same fish at the exact same time in the sequence. Lateral and ventral videos were calibrated in three dimensions using direct linear transformation (see Section 2.3). Each orange circle in the lateral view corresponds to an orange circle in the ventral view at the same location on the fin. These panels show 200 digitized points along the entire length of the anal fin. (C) Lateral view of the fish from the ninth frame of the backwards sequence and (D) ventral view of the same fish at the frame to show the digitizing of individual fin rays. Six points per fin ray for each of four fin rays near the middle of the anal fin were digitized.

Excel 2007 (Microsoft Corp., Redmond, WA, USA) for calculations of kinematic variables as described in Section 2.4.

2.4. Kinematic measurements

The following kinematic variables were calculated for each individual during each behavior: wave frequency, whole-fin wave amplitude, wave amplitude across the anterior half of the anal fin, wave amplitude across the posterior half of the anal fin, the ratio of the anterior amplitude to the posterior amplitude, whole-fin wavelength, wavelength across the anterior half of the anal fin, wavelength across the posterior half of the anal fin, the anterior to posterior wavelength ratio, the number of waves present along the fin, and horizontal and vertical velocity of the fish. Wave frequency was measured by taking the inverse of the period of an individual wave for each behavior. Wave amplitude was measured as the vertical distance between a peak and trough. Wavelength was measured as the horizontal distance between two successive peaks or troughs present on the anal fin. The total number of waves present on the fin was determined by counting the number of complete waves along the anal fin. Horizontal and vertical velocities of the fish were determined by tracking the horizontal and vertical changes in distance over time of the body point digitized on the nostril of each fish for each sequence.

2.5. Three-dimensional analysis of fin ray curvature

The radius of curvature (R) of an arc at a point is defined as the reciprocal of the absolute value of the curvature at that point (Protter and Morrey, 1970). In measuring the curvature of three points along a fin ray, a cyclic triangle can be formed. From this triangle, it is then possible to reconstruct a circumscribed circle with radius R and a curvature (and units) of $1/R$. Six evenly spaced points along four adjacent fin rays located in the middle of the anal fin were digitized in three dimensions to measure the fin ray curvature of two fish during each maneuver (Fig. 1C and D): points 1–6 from the proximal base of the fin to the distal tip. Whole fin ray curvature was estimated using points 1, 4, and 6 along each fin ray to give an average whole fin ray curvature. Basal fin ray curvature was measured from the three most basal points along each fin ray (points 1, 2, and 3). Distal fin ray curvature was measured from the three most distal points along each fin ray (points 4, 5, and 6). Fin ray curvature is presented here as the true three-dimensional curvature of the fin rays.

2.6. Statistical analysis

A canonical discriminant analysis (CDA) was performed to test multivariate differences among swimming maneuvers and to identify which anal fin kinematic variables were most useful for discriminating among swimming maneuvers (using JMP version 10; SAS Institute, Carey, NC, USA). Given a set of independent variables, discriminant analysis attempts to find linear combinations of those variables that best separate the groups of cases. CDA finds linear combinations of discriminating variables that maximize the differences among groups and minimize the differences within the groups (Dangles et al., 2005). For this analysis all anal fin kinematics except fin ray curvature were used. Fin ray curvature was not included in the analysis because data were collected from only two individuals. The Wilks' lambda test was used to determine if the differences explained by the discriminant variables were significant.

A two-way mixed-model ANOVA (using Systat v12; Systat Software, Inc., San Jose, CA, USA) was used to test globally for differences among individuals and behaviors (Table 1). Differences among maneuvers for each kinematic variable were determined using post hoc Student's t-tests.

3. Results

3.1. Anatomy of the ghost knifefish anal fin

The black ghost knifefish has a laterally compressed body with a deep profile that tapers in a blade-like fashion ventrally. Ghost knifefish retains a reduced caudal fin and paired pectoral fins; however, the anal fin is the most prominent fin on the body. It extends from the anteriorly located anus to the caudal fin, covering nearly three-quarters of the body length ventrally, and is composed of approximately 150 individual fin rays (varying from 140 to 160 in different individuals; Albert, 2001). Dorsal and pelvic fins are absent in ghost knifefish.

Micro CT imaging and cleared and stained specimens of knifefish revealed two notable skeletal features: extensive formation of intramuscular bones and a large modified haemal spine that projects anteriorly ventral to the body cavity (Fig. 2A and B). The

Table 1
Kinematic data for four swimming behaviors of ghost knifefish, *Apteronotus albifrons*, and analysis of statistical differences among the four behaviors. See text for definitions of variables and how each variable was measured. Values are overall means for each trial ± s.e. (standard error). Different letters indicate significant differences among maneuvers (see Section 2.6 for details of statistical analyses).

Variable	Backward	Forward	Heave	Hover
Wave frequency (Hz)[a]	5.19 ± 0.29^{B,C}	6.74 ± 0.73^{A}	6.33 ± 0.45^{A,B}	4.38 ± 0.34^{C}
Whole fin amplitude (cm)[a]	1.04 ± 0.04^{A}	1.12 ± 0.09^{A}	0.87 ± 0.03^{B}	0.87 ± 0.04^{B}
Anterior fin amplitude (cm)[a]	0.95 ± 0.05^{A}	0.95 ± 0.05^{A}	0.92 ± 0.03^{A}	0.94 ± 0.05^{A}
Posterior fin amplitude (cm)[a]	1.16 ± 0.05^{B}	1.38 ± 0.07^{A}	0.86 ± 0.0^{C}	0.82 ± 0.03^{C}
Ratio of anterior/posterior amplitude[a]	0.86 ± 0.04^{B}	0.70 ± 0.0^{C}	1.17 ± 0.07^{A}	1.17 ± 0.06^{A}
Wavelength (cm)[a]	3.03 ± 0.07^{A}	2.64 ± 0.18^{B}	2.68 ± 0.09^{B}	2.50 ± 0.11^{B}
Anterior wavelength (cm)	3.21 ± 0.07^{A}	2.7 ± 0.12^{B}	2.8 ± 0.09^{B}	2.65 ± 0.13^{B}
Posterior wavelength (cm)	2.9 ± 0.09^{B}	3.3 ± 0.14^{A}	2.6 ± 0.0^{C}	2.45 ± 0.12^{C}
Ratio of anterior/posterior wavelength	1.13 ± 0.03^{A}	0.83 ± 0.02^{B}	1.14 ± 0.05^{A}	1.13 ± 0.05^{A}
Distal fin ray curvature (cm^{-1})[b]	1.75 ± 0.15^{A}	1.43 ± 0.15^{A}	0.82 ± 0.10^{B}	1.74 ± 0.14^{A}
Basal fin ray curvature (cm^{-1})[b]	1.51 ± 0.16^{A,B}	1.59 ± 0.15^{A}	1.85 ± 0.27^{A}	1.10 ± 0.10^{B}
Fish horizontal velocity ($cm \times s^{-1}$)[a]	5.45 ± 0.30^{A}	–9.78 ± 1.0^{C,c}	0.39 ± 0.19^{B}	–0.45 ± 0.17^{B,c}
Fish vertical velocity ($cm \times s^{-1}$)[a]	–1.22 ± 0.22^{D}	1.50 ± 0.21^{B}	3.11 ± 0.33^{A}	0.08 ± 0.32^{C}
Number of waves[1]	3.10 ± 0.0^{C}	3.38 ± 0.12^{B}	3.88 ± 0.08^{A}	3.81 ± 0.12^{A}

[a] $n = 3$ individuals; 4 trials; each mean calculated from between 7 and 94 observations.
[b] $n = 2$ individuals; 4 trials; each mean calculated from between 7 and 94 observations.
[c] Forward motions along the *x*-axis are negative due to the anterior end of the fish facing left in all behaviors.

presence of so many intramuscular bones, formed from calcifications within the myosepta, may reflect a relatively high passive stiffness of the knifefish body.

The anal fin of the ghost knifefish is composed of fin rays, or lepidotrichia, enclosed within a thin fin membrane. As in other teleost fishes, each fin ray consists of two hemitrichs which have the ability to slide relative to each other like the halves of a bilaminar strip. Each hemitrich is further segmented into numerous small bony segments connected by collagen fibers. Anal fin rays either do not branch or only branch once near the distal end (Fig. 2C and D).

Muscles associated with the movement of the anal fin rays, from deep to superficial, include the mm. erectores anales, mm. depressores anales, and the mm. inclinatores anales (Fig. 2E; following the terminology of Winterbottom (1974) for ray-finned fish fin muscles). The mm. erectores anales and mm. depressores anales originate from the lateral faces of the basal pterygiophores of the anal fin and insert onto the anterior and posterior aspects of the fin ray base, respectively. The mm. inclinatores anales originate below the hypaxial body musculature and insert laterally on the proximal aspect of the fin ray.

3.2. Overview of whole fin kinematics

A. albifrons swims in different directions by passing undulatory waves along the anal fin from anterior to posterior, posterior to anterior, or in both directions simultaneously as inward-oriented counter-propagating waves. The supplementary video in the online Appendix provides a visual sense of the free and unconstrained swimming in this species where rapid changes in locomotor behaviors among forward, backward, hover, and heave locomotion occur frequently. To swim backwards, waves were predominantly generated from the posterior end of the fish and traveled anteriorly along the anal fin (Fig. 3A). During forward locomotion, waves were generated anteriorly and traveled posteriorly down the anal fin (Fig. 3B). In both heave and hover sequences, waves were generated at both the posterior and anterior ends of the fin and traveled inwards, ultimately colliding with one another (Fig. 3C and D). During these maneuvers, collisions ($n = 8$) always occurred between 0.25 and 0.75 of total anal fin length (AFL) with the anteriormost part of the anal fin defined as zero and the posterior end as 1. In a collision, the wave with a smaller amplitude and wavelength was absorbed by the larger wave, often resulting in a wave with a smaller amplitude but larger wavelength. Collisions also occurred in forward and backward maneuvers, with the collision always occurring at the opposite end of the anal fin to where the predominant waves were generated; in backward maneuvers, collisions ($n = 2$) occurred between 0.17 and 0.33 AFL, while in forward maneuvers ($n = 3$), they occurred between 0.76 and 0.91 AFL.

Table 1 provides mean values for variables measured from the anal fin, standard errors for those means, and a statistical comparison of differences among the different swimming behaviors. During unconstrained maneuvering locomotion, ghost knifefish swam forward at nearly twice the mean velocity of backwards swimming (Table 1). Backwards swimming was correlated with a slight downward motion of the body, whereas forwards swimming resulted in a similar upward body movement (Table 1). These correlated vertical movements occurred despite our deliberate selection of sequences that were as horizontal as possible. Posterior fin amplitude was significantly smaller in heave and hover behaviors than in backward and forward swimming (Table 1). Wavelength, especially anterior fin wavelength, was greatest in backwards swimming as compared to all other behaviors, whereas the ratio of anterior wavelength to posterior wavelength was lowest for forward swimming (Table 1).

The number of waves on the anal fin was significantly greater in both hovering and heave behaviors, compared to forward and backward locomotion (Table 1). Forward motion had a significantly greater number of anal fin waves than backward locomotion, and backward motion had a significantly longer overall wavelength; this was primarily due to the longer wave on the anterior region of the fin (Table 1).

The position of maximum amplitude and wavelength of the propagating wave along the anal fin was found to vary by swimming behavior. Backward and forward behaviors both exhibited the majority of their maximum amplitudes and wavelengths along the mid-section of the anal fin (approximately 0.33–0.67 AFL) (Fig. 4A and B). During backward swimming (Fig. 4A), 37% of the waves with maximum amplitude and 21% of waves with maximum wavelength occurred along the anterior half of the anal fin. In contrast, during forward swimming (Fig. 4B), 40% of the waves with maximum amplitude and 17% of waves with maximum wavelength occurred along the posterior half of the anal fin. Maximum amplitude and maximum wavelength were not coupled during a heave behavior, where the majority of waves with maximum amplitude occurred in the anterior half of the anal fin and the majority of waves with maximum wavelength occurred in the posterior half of the anal fin. While hovering, the majority of waves with maximum amplitude (88%) occurred in the anterior half of the anal fin and the majority of waves with maximum wavelength (65%) occurred across the mid-section of the anal fin.

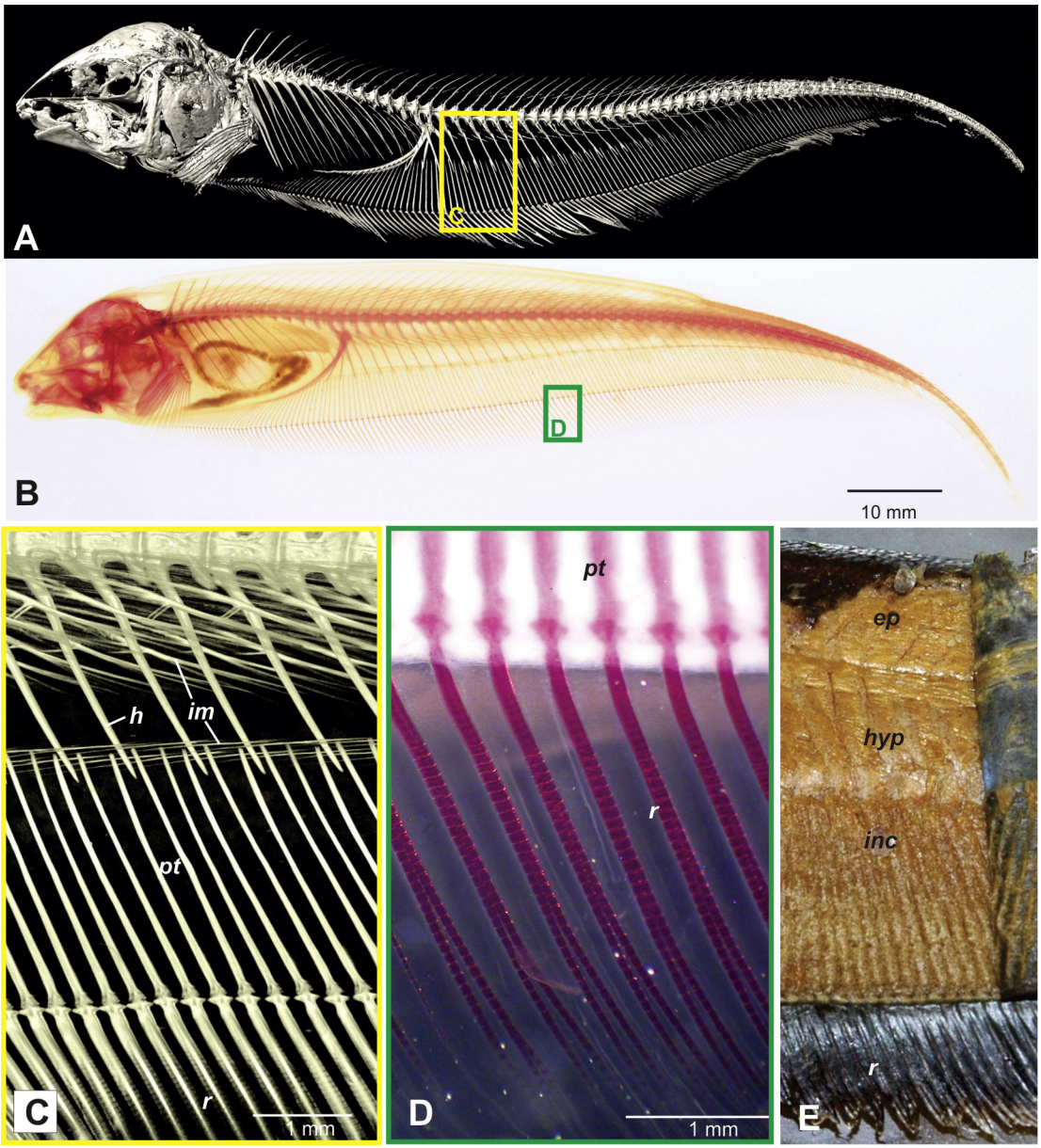

Fig. 2. Anatomy of ghost knifefish, *Apteronotus albifrons*. (A) Computed microtomography (micro CT) scan of a ghost knifefish specimen. (B) Cleared and stained specimen. (C) Close-up of the micro CT scan of knifefish, corresponding to the yellow box inset in (A). (D) Close-up of the cleared and stained specimen corresponding to the green inset in (B). (E) Superficial musculature of knifefish. Abbreviations: *ep*, epaxial muscle; *h*, hemal spine; *hyp*, hypaxial muscle; *im*, intramuscular bones; *inc*, inclinator muscles; *pt*, pterygiophore; *r*, anal fin rays.

Fig. 5 shows close-up views of individual fin rays at various locations along the length of the anal fin to demonstrate the considerable complexity of localized deformation that is achieved due to the numerous fin rays. In addition to the wave-like motion of the anal fin with broad peaks and valleys (Fig. 4), curvature and relative motion of fin rays can generate peaked configurations with relatively sharp crests as well as fin ray curling and curvature into oncoming flow (Fig. 5).

3.3. Fin ray curvature

Curvature of four adjacent fin rays located in the middle of the anal fin measured during a complete wave cycle showed that the greatest curvature occurred at the distal end of the fin rays (Fig. 6). Backward and forward swimming had similar patterns of fin ray curvature, with each peak in proximal curvature being preceded by a peak in distal curvature (Fig. 6A and B). Forward swimming resulted in the greatest maximum distal fin ray curvature (Fig. 6B; 4.5 cm^{-1}), but mean fin ray curvatures were not significantly different for forward and backward locomotion (Table 1). Heave and hover behaviors resulted in similar magnitude curvature of the distal part of the fin ray (Fig. 6C and D; approximately 3.5 cm^{-1}). Heave behavior resulted in a significantly lower distal fin ray curvature when compared to all other behaviors (Table 1). In hover behavior the basal fin ray curvature was significantly smaller than for heave and forward swimming but similar to that in backward locomotion (Table 1).

Maximum curvature of the four fin rays occurred at different times within a wave period during each behavior (Fig. 7). For most sequences, forward swimming had the greatest curvature for the longest amount of time for all four fin rays within a wave period. Greatest curvature of the fin rays occurred at 25% of the wave period during heave behaviors and at 100% of the period during hover behaviors.

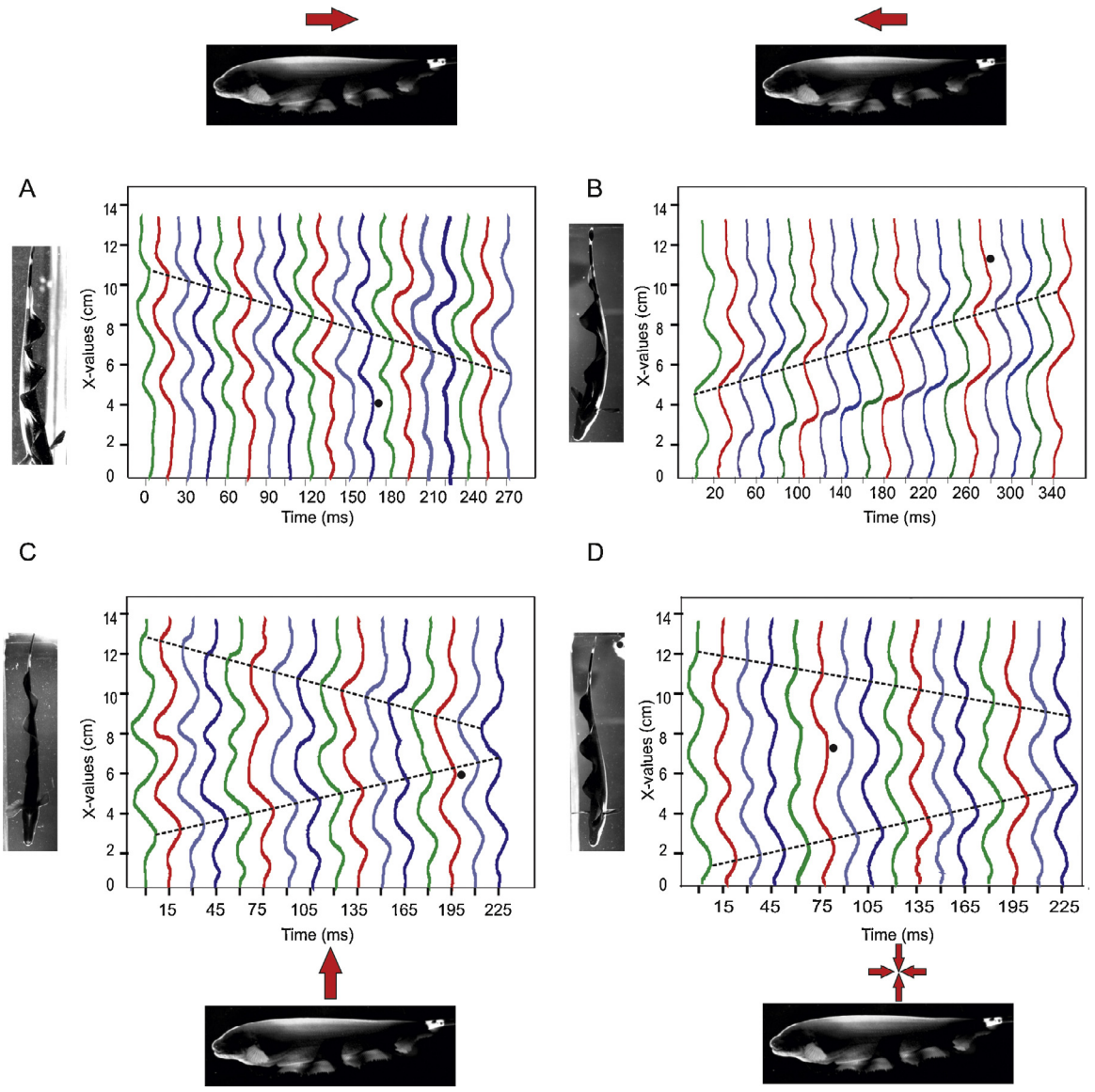

Fig. 3. Sinusoidal wave-like patterns of the anal fin during the knifefish's four swimming behaviors studied here: (A) backward swimming; (B) forward locomotion; (C) heave or upward motion; (D) hovering. Bold red arrows indicate the direction of body motion. Different colors designate sequential time steps and are used only to assist in tracking the wave movements. Dotted lines track the movement of one wave throughout the entire sequence. Black circles denote where a collision between two counter-propagating waves has occurred. In each collision, two counter-propagating waves are evident in the previous anal fin time point along the same region as the marked collision. Statistics for fin waveforms are given in Table 1.

Analysis of the curvature of a single fin ray during forward swimming (Fig. 8), obtained from six digitized points of one ray at 1 ms time intervals, illustrated that movement and curvature of this fin ray was initiated at the base of the ray and was trailed by the distal end, creating what resembles an S-wave. Such an S-wave is very pronounced at time 3, and two-dimensional outlines are projected onto the appropriate planes of the fin ray shape at this time (Fig. 8, lines 3a–c). Between time 3 and time 4 the distal end of the fin ray maintains a convex forward conformation even though it is moving in this direction, indicating that the fin ray is maintaining a concave curvature into the flow.

3.4. Multivariate statistical comparison among the four swimming behaviors

The first two discriminant functions of the canonical discriminant analysis had the greatest discriminating power, 98.9% (Table 2 and Fig. 9). These first two functions provided significant discrimination among groups ($P < 0.0001$), but the third discriminant function was not significant (Table 2). Anterior amplitude, posterior wavelength, whole-fin wavelength, ratio of anterior wavelength to posterior wavelength, wave frequency, and horizontal velocity were positively correlated with the first axis while the anterior wavelength, posterior amplitude, and ratio of anterior amplitude to posterior amplitude were negatively correlated. Wave number and vertical fish velocity were positively correlated with the second axis and the whole-fin amplitude was negatively correlated.

4. Discussion

4.1. Ghost knifefish fin kinematics

Ghost knifefish exhibit an extensive repertoire of locomotory modes, especially considering that the diversity of swimming behaviors is accomplished by modulating the undulation of a single

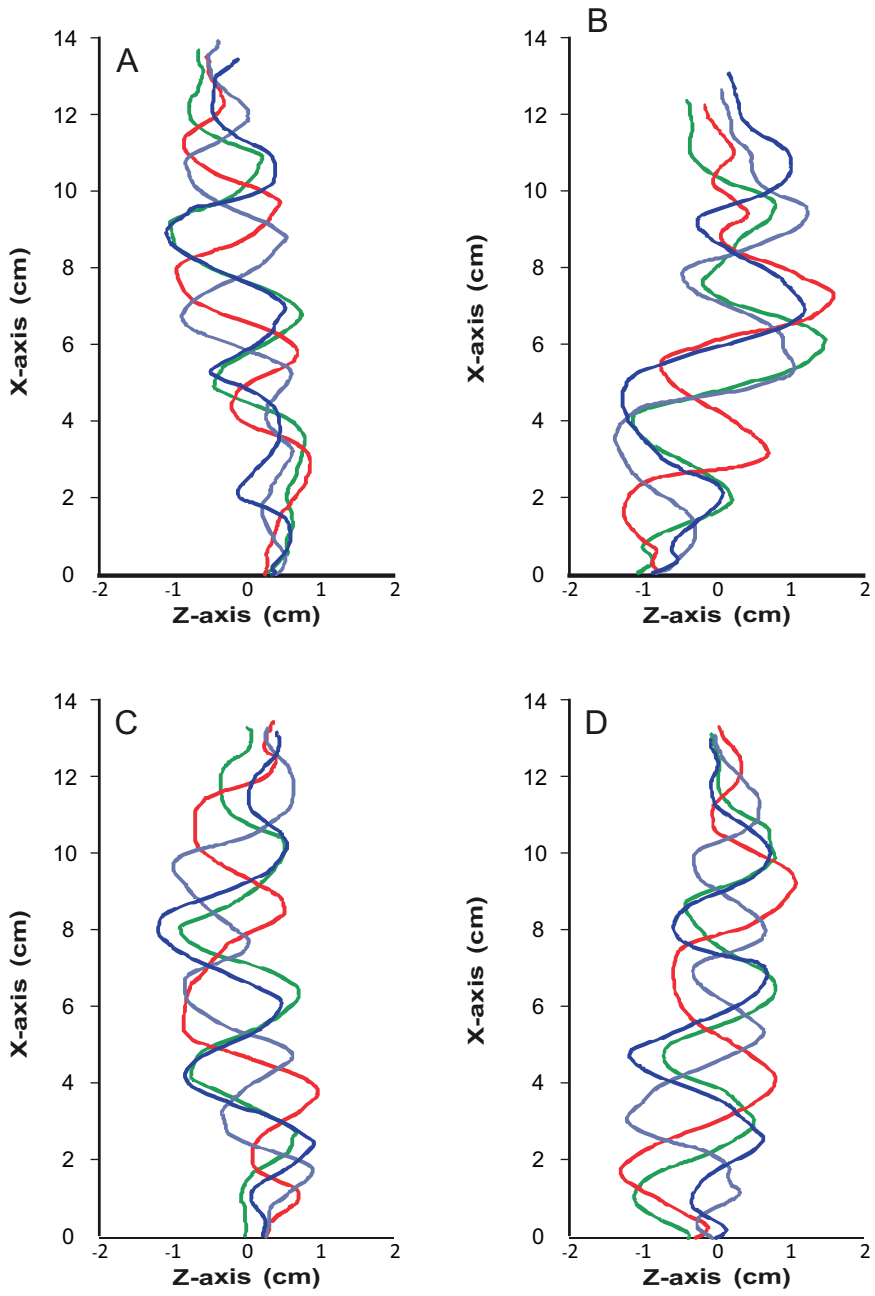

Fig. 4. Representative anal fin waveforms during one period of each swimming behavior: (A) backward swimming; (B) forward locomotion; (C) heave or upward motion; (D) hovering. The anterior-most part of the anal fin has a value of 0 on the *x*-axis. The green line represents the fin at the beginning of the period, the red line represents the fin at 1/3 of the period, the purple line represents the fin at 2/3 of the period, and the blue line represents the fin at the end of the period. Statistics for fin waveforms are given in Table 1.

fin. In addition to changing the direction of the undulatory wave to initiate forward or backward swimming, increasing the wavelength of the undulatory wave, particularly at the anterior end of the fin, was an important component of backward swimming. Also, changes in amplitude of fin undulations distinguished horizontal swimming from heave and hover behaviors (Table 1 and Fig. 9). It is worth noting that the body was held relatively stiff during backward and hover behaviors, while in forward and heave behaviors, the body did bend and may play a more active role in propulsion. As shown in Fig. 3, knifefish have the ability to change the direction, amplitude, number of waves, wavelength, and frequency of waves along their anal fin, and this kinematic flexibility is used to execute a diversity of locomotor behaviors and to transition rapidly among behaviors (see video in the online Appendix). Ghost knifefish also use their pectoral fins during free-swimming maneuvering, but the function of these fins and their possible role in contributing to motion of the body was not investigated here.

Fin ray curvature also varied by behavior: curvature was similar in magnitude along the length of the fin rays for forward and backward swimming, but greater at the proximal ends of the fin rays for heave behavior and at the distal end of the fin rays for hover behavior. Curvature of the fin ray is produced at the base by the inclinator muscles (Fig. 2), contraction of which causes the two hemitrichs of the fin ray to slide relative to each other, thus bending the whole fin ray (Alben et al., 2007; Lauder et al., 2011). Production of an "S"-shaped curve along an individual fin ray (Fig. 8; lines 3 and 4) requires differential activation of the left- and right-side inclinator muscles to bend the ray along its length. The location of

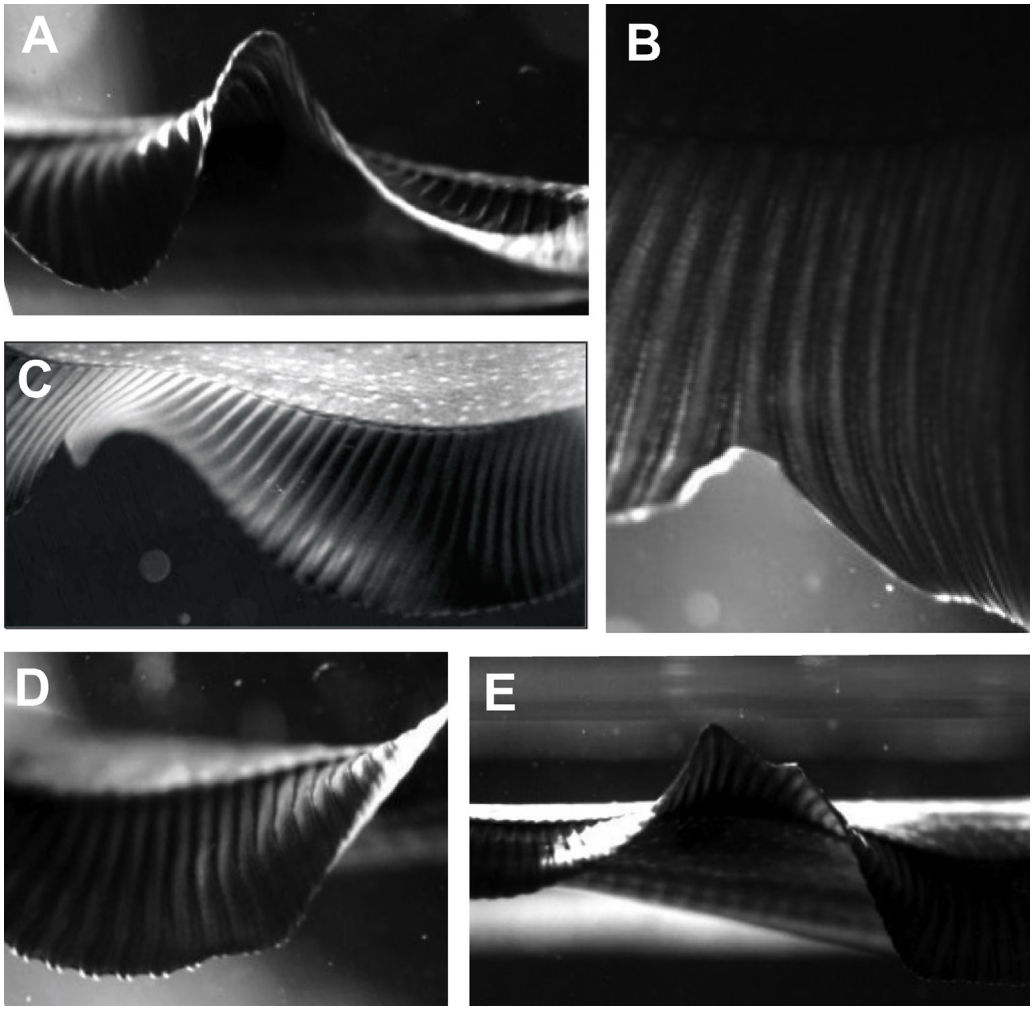

Fig. 5. Selected frames from 1000 fps high-speed video images of the ghost knifefish anal fin to show the diversity of fin ray conformations and bending patterns during free-swimming locomotor behaviors. Individual fin rays along the length of the anal fin are clearly visible. The anal fin, due to the numerous fin rays, may curve into complex shapes that include localized regions with (A) sharp and (B) shallow peaked configurations, (C) gently curved areas with (D) fin rays curling into the flow at the distal ends, and (E) intricate double-peaked profiles.

maximum curvature along the length of a fin ray can be manipulated by shifting the position of one hemitrich relative to the other before initiating bending (Alben et al., 2007; Lauder et al., 2011). Co-activation of the inclinator muscles, or use of the erector or depressor muscles, may help to stiffen the fin rays (Flammang and Lauder, 2008, 2009; Flammang et al., 2013) or alter the location of maximum curvature along the length of the ray (Geerlink and Videler, 1986).

The overall shape taken by fin rays during swimming is a result of the interplay between active forces generated by the inclinator musculature and the force on the fin that results from fluid loading. A purely passive fin and fin ray would be bent away from the direction of fluid motion, and would thus take a convex shape. But the ability to differentially move the two hemitrichs in each fin ray using the inclinator muscles allows teleost fin rays to oppose forces imposed by fluid loading. Such fin behaviors have been previously demonstrated for bluegill sunfish (Lauder and Madden, 2007), and now for the ghost knifefish anal fin where fin rays can be seen curving *into* the direction of motion and taking a concave shape (e.g., Fig. 8).

The results presented in Table 1 indicate that forward behaviors were best defined by a large posterior wavelength and large posterior amplitude while backward behaviors were best defined by a large anterior wavelength. The anterior fin amplitude data did not show a significant difference among different behaviors. Heave and hover behaviors offered an interesting contrast, although they were generally defined by similar kinematic variables (wave frequency, anterior amplitude, whole fin amplitude, and posterior wavelength): for each variable in this contrast, the mean values for heave were slightly greater than hover. These data suggest that hovering is the equivalent of a weakly executed heave motion with lower vertical force generation balanced by the weight of the fish body in water.

Curet et al. (2011a,b) investigated the counter propagating waves of the anal fin in *A. albifrons*, specifically those that occur during hover and heave behaviors, and analyzed the heave behavior in a robotic model of a knifefish anal fin. This style of ribbon fin movement has been termed “inward counter-propagating waves” and involves a series of traveling waves from the head to the tail, simultaneous with a series of traveling waves moving from tail to head. Our data are in concordance with their findings, and we also show that counter-propagating waves that collide along the fin length are present in forward and backward locomotor behaviors (Fig. 3). Such counter-propagating waves may act to control body position and also to produce behavioral combinations such as both forward and heave motions together, allowing the fish to

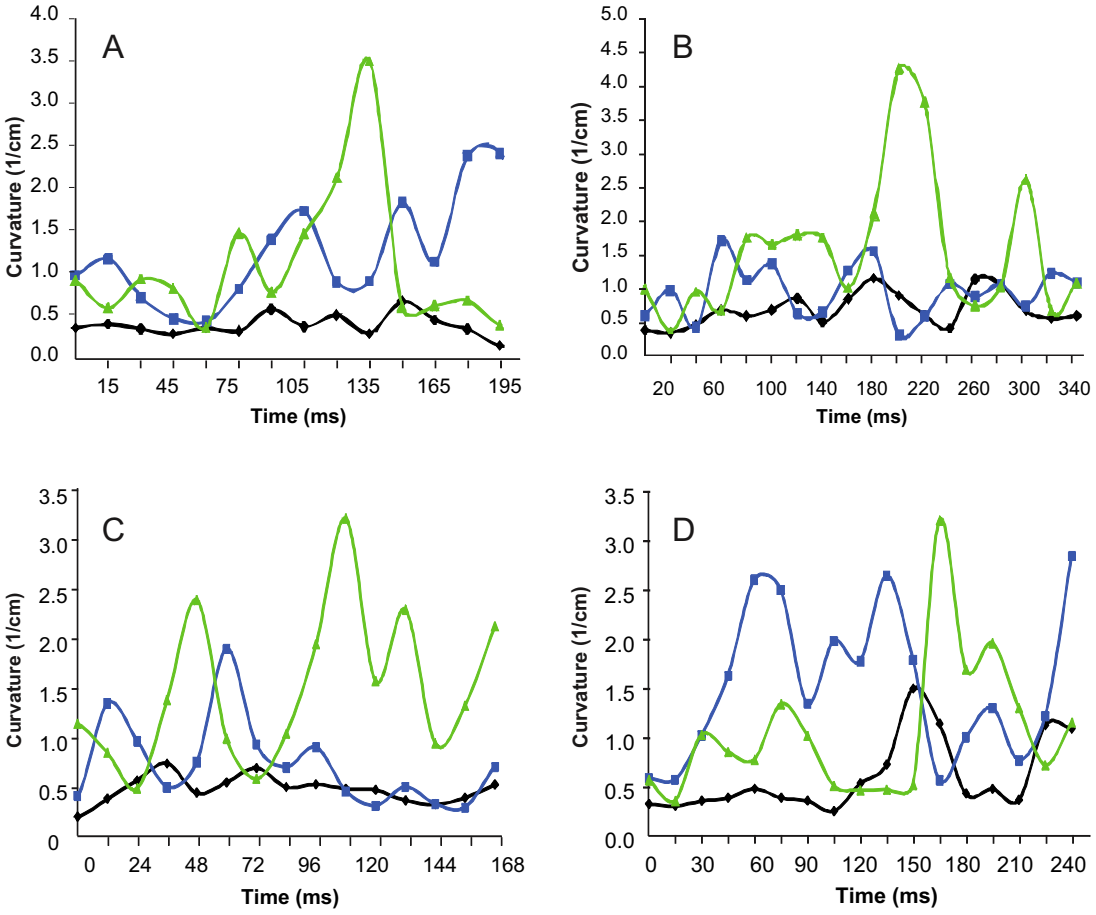

Fig. 6. Mean fin ray curvature of four adjacent fin rays during a complete wave cycle of the anal fin during four behaviors: (A) backward swimming; (B) forward locomotion; (C) heave or upward motion; (D) hovering. The black line represents the mean curvature of the entire fin ray, the blue line represents the mean curvature of the three most proximal points of the fin rays, and the green line represents the mean curvature of the three most distal points of the fin rays (see Section 2.5 for details of the measurement protocol). Statistics for fin ray curvature are given in Table 1.

move obliquely. In addition, Sefati et al. (2013), working with the glass knifefish, *Eigenmannia virescens*, recently demonstrated that for horizontal motion, colliding waves generate mutually opposing forces that simplify the control of body position. They showed that the use of counter-propagating waves increases the ability of the fish to stabilize the body, and to quickly initiate changes in body position.

4.2. Comparison of undulatory fin function among fishes

The ability of the ribbon-like anal fin in ghost knifefish to generate kinematic patterns that enhance body position control and also produce rapid changes in locomotor behavior is likely to be of particular importance for the free-swimming behaviors studied here. During free swimming, in contrast to controlled locomotion in a flow tank or tube, ghost knifefish rapidly transition among behaviors and explore the nearby environment using their electric sense to gather information on their immediate surroundings. As can be seen in the video in the online Appendix, free-swimming locomotion involves short-duration bursts of movement in the forward, backward, and heave directions, occasionally interrupted by momentary hovering events where body position changes minimally.

As a result of the dynamic nature of free swimming, we measure overall body velocities that are rarely seen in studies of steady rectilinear swimming in a flow tank where increased speeds are imposed on the fish and opportunities to avoid the flow are limited. For example, in this study we recorded mean forward and backward body velocities of about 10 cm s^{-1} and 5 cm s^{-1}, respectively (Table 1), compared to maximal tested swimming speeds of over 30 cm s^{-1} in studies of forward swimming in a flow tank (Ruiz-Torres et al., 2013). Our free-swimming forward speeds do correspond to the lower range of swimming speeds studied in Ruiz-Torres et al. (2013) who also report amplitude envelopes of fin motion and fin frequencies for these movements. Wavelengths of 2.5 cm recorded here for hovering are nearly equal to values from Ruiz-Torres et al. (2013), while the wavelengths during free-forward swimming are smaller than those reported for flow tank locomotion. However, our wavelengths for the posterior portion of the fin (Table 1) match well with the whole-fin values reported for forward locomotion at slower speeds.

Clades other than knifefishes within ray-finned fishes use fin undulations for propulsion and maneuvering (Blake, 1980; Jagnandan and Sanford, 2013); recent work by Jagnandan and Sanford (2013) reviewed the convergent evolution of ribbon-shaped fins in fishes: locomotion using elongate ribbon fins is found in a number of divergent phylogenetic clades. For example, bowfin (*Amia calva*) possess a long dorsal fin that allows locomotion using minimal body undulations at lower speeds, and Jagnandan and Sanford (2013) quantified the wavelengths on the anterior and posterior regions of this fin during forward swimming as well as wave speed and frequency of undulation in a similar manner to our

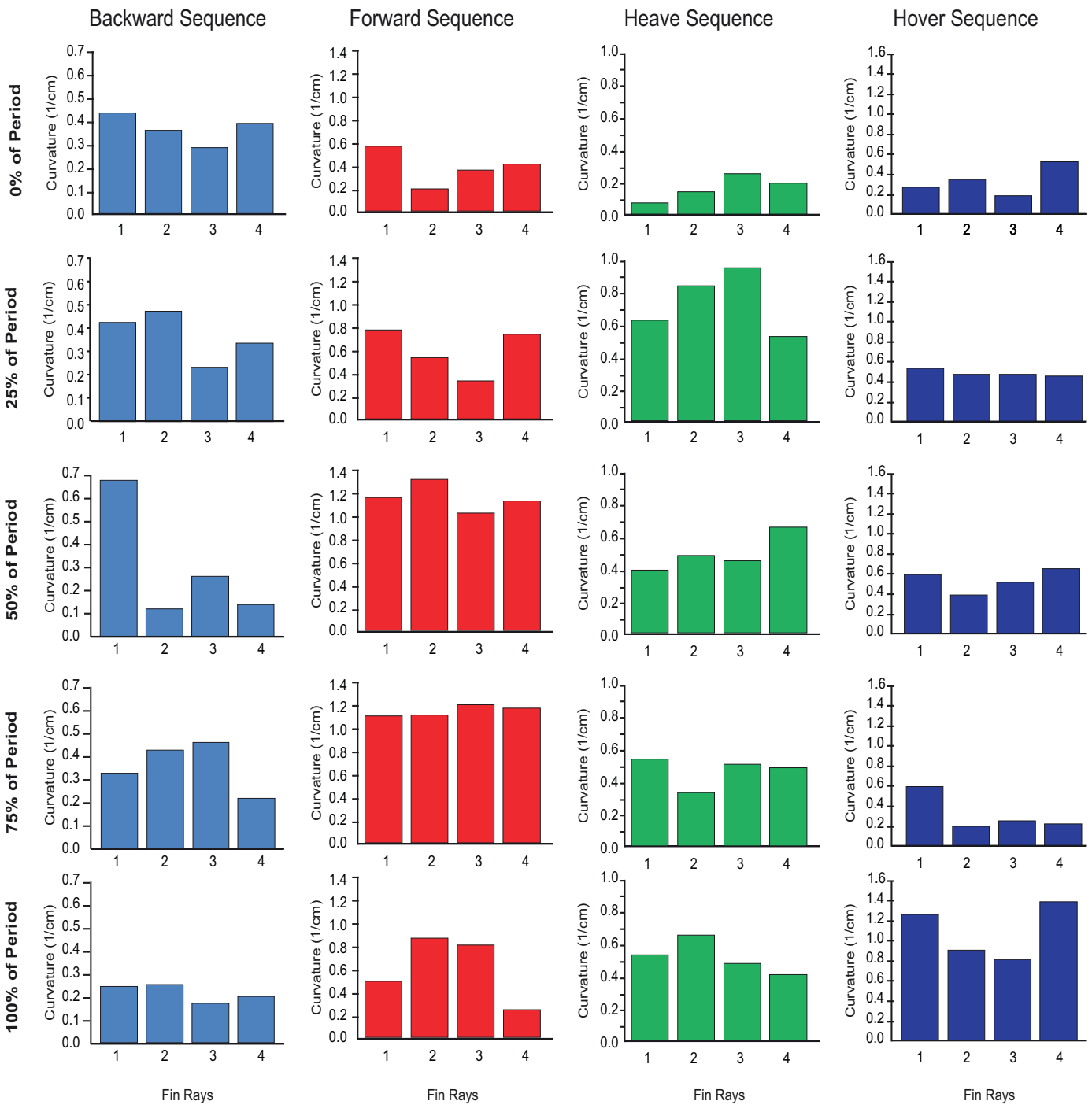

Fig. 7. Curvature of individual fin rays. Fin rays are plotted on the *x*-axis with ray 1 being the most anterior along the fin; rays 2–4 are located posteriorly in order. These four fin rays were located in the middle of the anal fin. Each graph represents a single period of time during the sequence. Statistics for fin ray curvatures are given in Table 1.

methods here. Ghost knifefish used much higher fin frequencies (4–6 Hz; Table 1) than did bowfin (2–3 Hz) and this may be due in part to the larger body size of the bowfin which averaged 30 cm long, and to increased use of body undulatory motion by bowfin as swimming speed increases.

4.3. Comparison of fin ray curvatures among fishes

In addition to measuring the canonical locomotor parameters that characterize undulatory bodies or fins such as wave amplitude, frequency, and wavelength, it is important to quantify details of how individual fin rays within the fin are moving. Since it is the fin surface that interacts with the water to generate locomotor forces, determining the shape of that fin surface is an important component of understanding fin-based locomotion. With approximately 150 fin rays in the ghost knifefish anal fin, it is not possible to measure the motion of all fin rays. A camera view that provides a view of the whole fin is not able to visualize individual fin rays and show ray conformation during swimming (Figs. 5 and 8), and so we concentrated on four fin rays in the middle

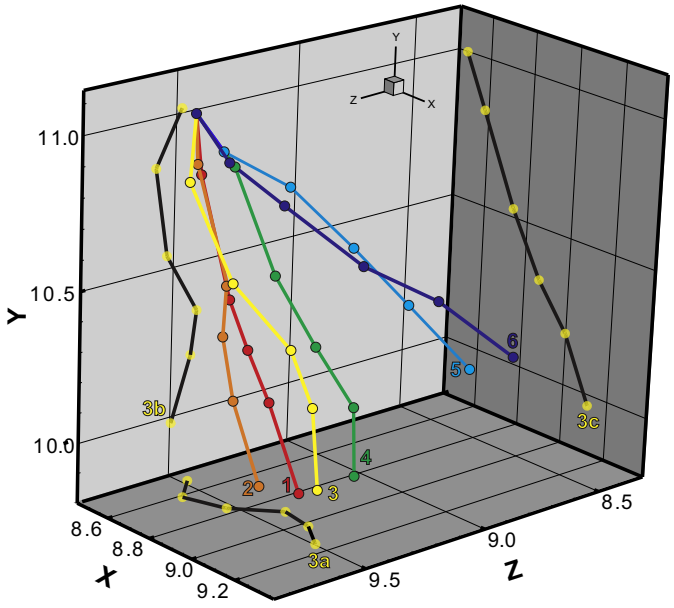

Fig. 8. Three-dimensional plot of the motion of one individual fin ray, located in the middle of the anal fin, during forward swimming at six time steps (progressing from 1 to 6), 1 ms apart. The fin ray at time 3 (yellow) is projected onto the *XZ*, *ZY*, and *XY* planes (3a, 3b, and 3c, black lines with yellow nodes) to illustrate the three-dimensional nature of fin ray curvature. The base of the ray is located at the upper left where the colored lines converge. Note that portions of the fin ray are convexly curved in the direction of motion, indicating active control of fin ray curvature. Units on each axis are millimeters.

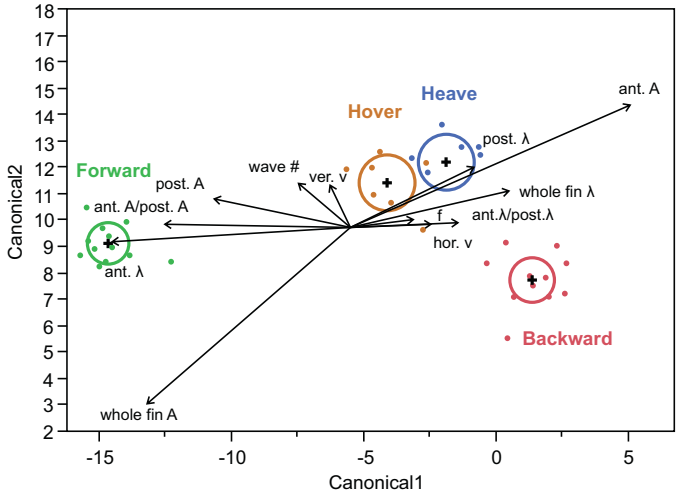

Fig. 9. Canonical discriminant analysis of the four swimming behaviors in ghost knifefish based on anal fin kinematics. See Section 2.6 for further discussion of this analysis. The size of each circle corresponds to a 95% confidence limit for the mean for each behavior which is indicated by the black cross. Vectors indicate the direction and magnitude of the loading of each variable in the discriminant space. Each vector is labeled with the corresponding variable (Table 1). Table 2 provides the statistical analysis of the data presented here. Abbreviations: *A*, amplitude of motion, *v*, velocity; λ, wavelength.

of the anal fin (Fig. 1C and D) as a focal group of fin rays to study in detail.

Our results demonstrate that ghost knifefish are actively curving their fin rays. This was found to be the case in all of the fish studied and in each behavior analyzed. Fig. 8 demonstrates the sequence of one fin ray through time. Starting from $t = 1$, it is clear that the fish is actively curving the basal portion of its fin ray against the water and the distal end of the fin ray follows, passively curving in the opposite direction of the basal end as a result of the force from the water acting on the fin. The resulting fin ray shape resembles an "S". This helps explain our results presented in Fig. 6 in which both the basal curvature and the distal curvature values at any point in time are greater than the entire fin ray curvature values. The curvature of the entire fin ray, although an accurate measurement of the curvature between three points, measures the fin ray as though it is an arc and not an S-wave. Hence, the values of curvature for the entire fin ray should be less than for the basal or distal curvature values alone, if at the time of measurement the fin ray resembles an S-wave. The significance of fin ray curvature for hydrodynamic function of the fin has yet to be studied in detail, but the effect produced when individual fin rays curve into oncoming flow is to cause the entire fin surface to bend into the flow. Lauder and Madden (2007) show an image of the pectoral fin from a bluegill sunfish with the fin surface curved into the flow during a turning maneuver. Based on manipulations of robotic fish fins which allow fin stiffening and curvature parameters to be altered and forces measured, changing fin stiffness and hence fin ray curvature can enhance locomotor forces, and when the fin is "cupped" or curved into the flow, thrust can be increased (Tangorra et al., 2010; Esposito et al., 2012).

Fin rays show different curvatures from base to tip and different positions relative to their base throughout a sequence of movement. Curvature values even between adjacent fin rays can be quite different. A clear example of this can be seen in Fig. 7; rays 1, 2, 3 and 4 all display different curvatures, suggesting that they have some level of independence from one another despite being connected by a flexible membrane. As the present study only looked at the curvature of four of the 150 fin rays of the anal fin, further data collection is required to determine if the fin rays of the entire fin also exhibit some level of independence from one another.

The values for maximal fin ray curvature presented in this paper are substantially higher than previously measured literature values (Table 3). The values obtained were more than twice the value of previously known maximum curvature values found in the pectoral fins of the sculpin, *Myoxocephalus octodecimspinosus* (Taft et al., 2008), and more than 10 times the values seen in free-swimming bluegill sunfish. Ghost knifefish maximal fin ray curvatures during free swimming were even greater than fin ray curvatures reported for the escape response of bluegill sunfish (Chadwell et al., 2012), and more than double the fin ray curvatures produced by deformation of pectoral fin rays as a result of experiments in which vortex rings were aimed at pectoral fins of bluegill sunfish (Flammang et al., 2013). These large fin ray curvatures in ghost knifefish may be a function of (i) fin ray mechanical design that differs in this species from those studied previously and allows greater bending, (ii) greater actuation or relative muscle mass of inclinator musculature that produces fin ray bending, or (iii) some combination of the above. Regardless of the cause, the ability of ghost knifefish to bend their anal fin rays to a much greater extent than previously

Table 2
Results for the three discriminant functions of the discriminant canonical analyses of locomotor behaviors. The first two discriminating functions are presented in graphical form in Fig. 9.

Discriminant function	Eigenvalue	Cumulative percent	Canonical correlation	Wilks' Lambda	Probability
1	49.7	92.5	0.99	0.003	<0.0001
2	3.4	98.9	0.88	0.141	<0.0001
3	0.59	100	0.61	0.627	0.21

Table 3
Comparative fin ray curvature data from the present paper and the literature for ray-finned fish fins used during locomotion.

Fish (species)	Fin	Maximum curvature (mm^{-1})	Source
Black ghost knifefish (*Apteronotus albifrons*)	Anal	0.78	Present paper
Bluegill sunfish (*Lepomis macrochirus*)	Anal	0.08	Standen and Lauder (2005)
	Dorsal	0.09	Standen and Lauder (2005)
	Pectoral	0.30	Flammang et al. (2013)
(c-start)	Dorsal	0.28	Chadwell et al. (2012)
(c-start)	Anal	0.25	Chadwell et al. (2012)
Longhorn sculpin (*Myoxocephalus octodecimspinosus*)	Pectoral	0.45	Taft et al. (2008)

reported for other species suggests that further investigation of the effects of bending on locomotor performance is warranted.

Acknowledgements

We thank J. McConnell, S. Gandiaga, and W. Goldsmith for assistance with fish care. J. McConnell was also instrumental in data collection and analysis. Special thanks to Malcolm MacIver, Neelesh Patankar, and Noah Cowan for many discussions and for collaborative research on knifefish locomotion. Funding was provided by the National Science Foundation (grants EFRI-0938043 and CDI 0941674).

Appendix A. Supplementary data

Supplementary material related to this article can be found, in the online version, at http://dx.doi.org/10.1016/j.zool.2014.04.004.

References

Alben, S., Madden, P.G., Lauder, G.V., 2007. The mechanics of active fin-shape control in ray-finned fishes. J. Roy. Soc. Inter. 4, 243–256.
Albert, J.S., 2001. Species diversity and phylogenetic systematics of American knifefishes (Gymnotiformes, Teleostei). Misc. Publ. Mus. Zool. Univ. Michigan 190, 1–127.
Blake, R.W., 1980. Undulatory median fin propulsion of two teleosts with different modes of life. Can. J. Zool. 58, 2116–2119.
Blake, R.W., 1983. Swimming in the electric eels and knifefishes. Can. J. Zool. 61, 1432–1441.
Blevins, E., Lauder, G.V., 2012. Rajiform locomotion: three-dimensional kinematics of the pectoral fin surface during swimming by the freshwater stingray *Potamotrygon orbignyi*. J. Exp. Biol. 215, 3231–3241.
Chadwell, B.A., Standen, E.M., Lauder, G.V., Ashley-Ross, M.A., 2012. Median fin function during the escape response of bluegill sunfish (*Lepomis macrochirus*). II. Fin-ray curvature. J. Exp. Biol. 215, 2881–2890.
Curet, O.M., Patankar, N.A., Lauder, G.V., MacIver, M.A., 2011a. Aquatic manoeuvering with counter-propagating waves: a novel locomotive strategy. J. Roy. Soc. Inter. 8, 1041–1050.
Curet, O.M., Patankar, N.A., Lauder, G.V., MacIver, M.A., 2011b. Mechanical properties of a bio-inspired robotic knifefish with an undulatory propulsor. Bioinsp. Biomimet. 6, http://dx.doi.org/10.1088/1748-3182/6/2/026004.
Dangles, O., Magal, C., Pierre, D., Olivier, A., Casas, J., 2005. Variation in morphology and performance of predator-sensing system in wild cricket populations. J. Exp. Biol. 208, 461–468.
Esposito, C., Tangorra, J., Flammang, B.E., Lauder, G.V., 2012. A robotic fish caudal fin: effects of stiffness and motor program on locomotor performance. J. Exp. Biol. 215, 56–67.
Flammang, B.E., Lauder, G.V., 2008. Speed-dependent intrinsic caudal fin muscle recruitment during steady swimming in bluegill sunfish, *Lepomis macrochirus*. J. Exp. Biol. 211, 587–598.
Flammang, B.E., Lauder, G.V., 2009. Caudal fin shape modulation and control during acceleration, braking and backing maneuvers in bluegill sunfish, *Lepomis macrochirus*. J. Exp. Biol. 212, 277–286.
Flammang, B.E., Alben, S., Madden, P.G.A., Lauder, G.V., 2013. Functional morphology of the fin rays of teleost fishes. J. Morphol. 274, 1044–1059.
Geerlink, P.J., Videler, J.J., 1986. The relation between structure and bending properties of teleost fin rays. Neth. J. Zool. 37, 59–80.
Hedrick, T.L., 2008. Software techniques for two- and three-dimensional kinematic measurements of biological and biomimetic systems. Bioinsp. Biomim. 3, 034001.
Hu, T., Shen, L., Lin, L., Xu, H., 2009. Biological inspirations, kinematics modeling, mechanism design and experiments on an undulating robotic fin inspired by *Gymnarchus niloticus*. Mech. Mach. Theor. 44, 633–645.
Jagnandan, K., Sanford, C.P., 2013. Kinematics of ribbon-fin locomotion in the bowfin, *Amia calva*. J. Exp. Zool. A 319, 569–583.
Lauder, G.V., Drucker, E.G., 2004. Morphology and experimental hydrodynamics of fish fin control surfaces. IEEE J. Ocean. Eng. 29, 556–571.
Lauder, G.V., Madden, P.G.A., 2007. Fish locomotion: kinematics and hydrodynamics of flexible foil-like fins. Exp. Fluids 43, 641–653.
Lauder, G.V., Madden, P.G.A., Mittal, R., Dong, H., Bozkurttas, M., 2006. Locomotion with flexible propulsors. I. Experimental analysis of pectoral fin swimming in sunfish. Bioinsp. Biomimet. 1, S25–S34.
Lauder, G.V., Madden, P.G.A., Tangorra, J., Anderson, E., Baker, T.V., 2011. Bioinspiration from fish for smart material design and function. Smart Mater. Struct. 20, http://dx.doi.org/10.1088/0964-1726/20/9/094014.
Lighthill, J., 1990. Biofluiddynamics of balistiform and gymnotiform locomotion. Part 3. Momentum enhancement in the presence of a body of elliptic cross-section. J. Fluid Mech. 213, 11–20.
Lighthill, J., Blake, R., 1990. Biofluiddynamics of balistiform and gymnotiform locomotion. Part 1. Biological background and analysis by elongated-body theory. J. Fluid Mech. 212, 183–207.
Low, K.H., Willy, A., 2006. Biomimetic motion planning of an undulating robotic fish fin. J. Vibr. Contr. 12, 1337–1359.
MacIver, M.A., Sharabash, N.M., Nelson, M.E., 2001. Prey-capture behavior in gymnotid electric fish: motion analysis and effects of water conductivity. J. Exp. Biol. 204, 543–557.
MacIver, M.A., Fontaine, E., Burdick, J.W., 2004. Designing future underwater vehicles: principles and mechanisms of the weakly electric fish. IEEE J. Ocean. Eng. 29, 651–659.
McCutchen, C.W., 1970. The trout tail fin: a self-cambering hydrofoil. J. Biomech. 3, 271–281.
Neveln, I.D., Bai, Y., Snyder, J.B., Solberg, J.R., Curet, O.M., Lynch, K.M., MacIver, M.A., 2013. Biomimetic and bio-inspired robotics in electric fish research. J. Exp. Biol. 216, 2501–2514.
Neveln, I.D., Bale, R., Bhalla, A.P.S., Curet, O.M., Patankar, N.A., MacIver, M.A., 2014. Undulating fins produce off-axis thrust and flow structures. J. Exp. Biol. 217, 201–213.
Protter, M.H., Morrey, C.B., 1970. Calculus with Analytic Geometry: A First Course. Addison Wesley Publishing Co., Reading, MA.
Ruiz-Torres, R., Curet, O.M., Lauder, G.V., MacIver, M.A., 2013. Kinematics of the ribbon fin in hovering and swimming of the electric ghost knifefish. J. Exp. Biol. 216, 823–834.
Sefati, S., Neveln, I.D., Roth, E., Mitchell, T.R.T., Snyder, J.B., MacIver, M.A., Fortune, E.S., Cowan, N.J., 2013. Mutually opposing forces during locomotion can eliminate the tradeoff between maneuverability and stability. Proc. Natl. Acad. Sci. U.S.A. 110, 18798–18803.
Shirgaonkar, A.A., Curet, O.M., Patankar, N.A., MacIver, M.A., 2008. The hydrodynamics of ribbon-fin propulsion during impulsive motion. J. Exp. Biol. 211, 3490–3503.
Standen, E.M., Lauder, G.V., 2005. Dorsal and anal fin function in bluegill sunfish *Lepomis macrochirus*: three-dimensional kinematics during propulsion and maneuvering. J. Exp. Biol. 208, 2753–2763.
Taft, N.K., Taft, B.N., 2012. Functional implications of morphological specializations among the pectoral fin rays of the benthic longhorn sculpin. J. Exp. Biol. 215, 2703–2710.
Taft, N., Lauder, G.V., Madden, P.G., 2008. Functional regionalization of the pectoral fin of the benthic longhorn sculpin during station holding and swimming. J. Zool. Lond. 276, 159–167.
Tangorra, J.L., Lauder, G.V., Hunter, I., Mittal, R., Madden, P.G., Bozkurttas, M., 2010. The effect of fin ray flexural rigidity on the propulsive forces generated by a biorobotic fish pectoral fin. J. Exp. Biol. 213, 4043–4054.
Winterbottom, R., 1974. A descriptive synonymy of the striated muscles of the Teleostei. Proc. Acad. Nat. Sci. Phil. 125, 225–317.